

Spreading of a density front in the Küntz-Lavallée model of porous media

Maciej Matyka and Zbigniew Koza

Institute of Theoretical Physics, University of Wrocław, pl. Maksa Born 9, 50-204 Wrocław, Poland,

E-mail: maq@ift.uni.wroc.pl

Abstract. We analyze spreading of a density front in the Küntz-Lavallée model of porous media. In contrast to previous studies, where unusual properties of the front were attributed to anomalous diffusion, we find that the front evolution is controlled by normal diffusion and hydrodynamic flow, the latter being responsible for apparent enhancement of the front propagation speed. Our finding suggests that results of several recent experiments on porous media, where anomalous diffusion was reported based on the density front propagation analysis, should be reconsidered to verify the role of a fluid flow.

Submitted to: *J. Phys. D: Appl. Phys.*

1. Introduction

The root-mean-square displacement, $\sqrt{\langle r^2 \rangle}$, of a single diffusing particle at long times t is typically proportional to t^α with $\alpha = 1/2$. The same scaling law is also usually obeyed by the width of a region infiltrated by a diffusing front. However, there are also many natural phenomena where the exponent α differs from $1/2$. These include, for example, water absorption in porous building materials [1, 2, 3, 4], copper sulfate diffusion into deionized water [5, 6], transport in high polymer systems [7], diffusion through synthetic membranes [8], and some aspects of surface diffusion [9]. Diffusion processes with $\alpha = 1/2$ are ubiquitous in Nature and hence called ‘normal’, whereas those with $\alpha \neq 1/2$ are quite rare and called ‘anomalous’.

There are several mechanisms that are known to bring about anomalous tracer [10] diffusion; for example, a power-law probability distribution of waiting times between individual steps of a random walk or a power-law probability distribution of distances covered by the diffusing particle at each jump [11, 12]. However, far less is known about anomalous chemical [10] diffusion, i.e. diffusion of macroscopic quantities of matter. Anomalous spreading of diffusion fronts is a many-body effect that results from complicated interactions between diffusing particles as well as between the particles and the surrounding (e.g. porous or fractal-like) medium. In many cases the nature of these

interactions remains unknown, so actually there is no satisfactory explanation of the anomalous diffusion in these systems [9]. Thus, any progress in the theory of anomalous chemical diffusion would be much welcomed.

Recently Küntz and Lavallée [6, 13, 14] suggested that anomalous chemical diffusion can be a common phenomenon in systems with concentration-dependent diffusion coefficient of the diffusing entity. They based it on extensive computer simulations of a lattice-gas automata (LGA) model [13, 14], and a refined analysis of a CuSO_4 front diffusion into deionized water experiment [6]. Were this conjecture correct, it could be used to identify the cause of anomalous spreading of concentration fronts in many real systems.

In this paper we focus on the Küntz and Lavallée (KL) model and propose a much simpler interpretation of the simulation results obtained in [13, 14]. Our approach indicates that the diffusion in the KL model is normal. The key to the proper interpretation of the simulation results is the fact that the KL model is an extension of the Frish-Hasslacher-Pomeau (FHP) lattice gas model of fluid flow. Even though Küntz and Lavallée applied it in a porous medium, which significantly reduced the flow velocity, hydrodynamic effects were not eliminated altogether. We found that the fluid flow velocity is large enough to enhance the effective speed of the diffusing front, apparently enlarging the value of the scaling exponent α above $1/2$. We show that when the flow is taken into account, the exponent α assumes its expected, “normal” value $1/2$.

In a broader perspective, our study shows that application of “hydrodynamic” lattice-gas automata models to study diffusion in porous media requires a great caution. Special attention must be paid to modelling the porosity of the medium to ensure that there is no macroscopic flow through the system. If this is impossible, the flow, even of minute magnitude, must be explicitly taken into account in the analysis of results.

The structure of the paper is as follows. In Section 2 we briefly introduce the Küntz-Lavallée model and the main results obtained thus far. In Section 3 we present our interpretation of these results, and show that actually there is no anomalous diffusion in the system. Section 4 presents discussion of the major properties of the model. Finally, Section 5 is devoted to conclusions.

2. The Küntz-Lavallée model

The Küntz-Lavallée model [6, 13, 14, 15] describes diffusion of a fluid in a porous medium and is an extension of a deterministic Frish-Hasslacher-Pomeau (FHP₅) lattice-gas automata model of fluid flow [16]. The system is reduced to a two-dimensional triangular lattice, L_x lattice units (l.u.) long and $L_y\sqrt{3}/2$ l.u. wide. The total number of lattice nodes is thus $N = L_x L_y$. They are occupied by indistinguishable particles, whose velocities belong to a discrete, 7-element set (Fig. 1). Any particles occupying the same lattice site must have different velocities, so that each node can be occupied by at most 7 particles. The time is discrete and at each time step particles either stay

at rest (if their speed is 0) or jump to the adjacent site pointed at by their velocity vector. Particles arriving simultaneously at the same node may collide. The collision rules for the FHP₅ model are depicted in Fig. 1; they conserve the mass and momentum. Additionally, a porous medium is modelled by assuming that a fraction c_s of randomly chosen lattice nodes is permanently occupied by the so called specular scatterers (such scatterers behave like tiny rigid squares parallel to the “x” axis [15]). The system is confined between rigid, impenetrable walls along the “x” direction, whereas periodic boundary conditions are assumed along the “y” direction. A characteristic feature of the model thus constructed is a strong dependence of the diffusion coefficient D on the reduced local particle concentration c [13], which is defined as the average number of particles per node divided by 7. It turns out that D assumes a minimum value at $c \approx 0.2$ and diverges to infinity as c goes either to 0 or 1 [13].

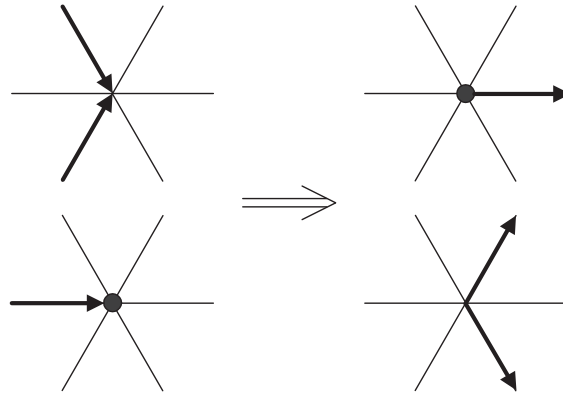


Figure 1. Collision rules in the FHP₅ model. Filled circles represent particles at rest.

Initially the system is uniformly filled with particles so that the reduced concentration is c_2 throughout the system. To this end $7c_2N$ particles are distributed randomly in the system in such a way that their mean velocity vanishes and any particles occupying the same node have different velocities. Next, a narrow strip of nodes at the left-hand side of the system is uniformly filled with additional particles so as to increase the reduced concentration to $c_1 > c_2$. In this way a step-like nonuniform initial condition is formed,

$$c(x, 0) = c_1 H(-x), \quad x < 0, \quad c(x, 0) = c_2 H(x), \quad x > 0, \quad (1)$$

where $H(x)$ is the Heviside step function. The origin of the reference system is set to the interface between the areas of high and low initial concentration, so that $x = 0$ corresponds to the initial location of the step.

During the simulation, by injecting new particles if necessary, the reduced concentration in the boundary strip $x < 0$ is maintained fixed at c_1 . This corresponds to boundary conditions that are often used in studies on water infiltration into a porous medium:

$$c(x, t) = c_1 \text{ for } x = 0, \quad c(x, t) \rightarrow c_2 \text{ as } x \rightarrow \infty. \quad (2)$$

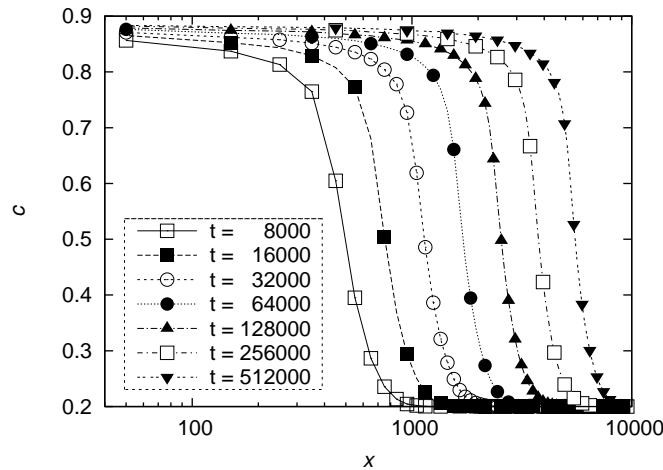


Figure 2. Reduced concentration profile $c(x, t)$ as a function of position x for $t = 8000 \times 2^k$ time steps, $k = 0, 1, \dots, 6$. The boundary conditions are $c_1 = 0.9$ and $c_2 = 0.2$.

3. Results

We performed extensive simulations of a concentration front propagation using a triangular lattice with $L_x = 8000$, $L_y = 200$, the density of scatterers $c_s = 0.08$, and the initial and boundary conditions determined by $c_1 = 0.9$ and $c_2 = 0.2$. The results for $t = 8000 \times 2^k$, $k = 0, 1, \dots, 6$, are depicted in Figure 2 as a semi-logarithmic plot. Both the shape of the consecutive curves and the distances between them appear to be almost the same, which suggests that the concentration profile $c(x, t)$ can actually be expressed as a function of a single variable x/t^α .

Validity of the scaling hypothesis can be verified by plotting several concentration profiles, obtained at different times, as functions of x/t^α . If the scaling holds, all these plots should collapse into a single curve. Such analysis was already performed in [13], where it was found that $\alpha \approx 0.55$. This was interpreted as an evidence that the transport in the LGA model is superdiffusive ($\alpha > 1/2$).

This finding, however, leads to a paradox: how addition of scatterers can *enhance* transport of particles? According to Küntz and Lavallée [13], this paradox can be explained by two hypotheses. The first one attributes superdiffusion of particles to a very strong dependence of their diffusivity on concentration. The second one says that anomalous diffusion is actually a transient phenomenon: in the limit of time $t \rightarrow \infty$ the scaling exponent α will *extremely slowly* decrease to $1/2$.

However, this argumentation neglects a well known fact, widely used in the Boltzmann-Matano method [10, 17], that any solution to the diffusion equation

$$\frac{\partial c(x, t)}{\partial t} = \frac{\partial}{\partial x} \left(D(c) \frac{\partial c(x, t)}{\partial x} \right), \quad (3)$$

with the initial and boundary conditions (1) and (2), satisfy the $x/t^{1/2}$ scaling for all t , irrespective of the form of $D(c)$ [17]. Consequently, absence of this scaling indicates

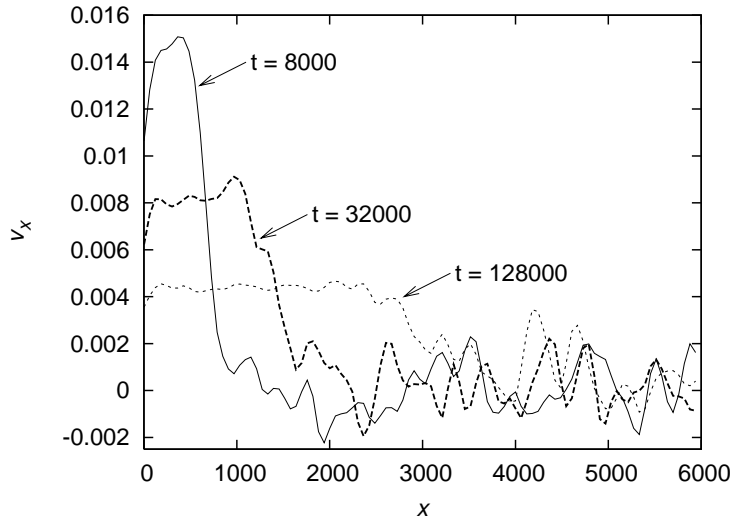


Figure 3. The “x” component of the velocity, v_x , as a function of the distance from the origin, x , for time $t = 8000 \times 4^k$, $k = 0, 1, 2$.

that equation (3) cannot give a proper description of the concentration front dynamics in the model. Besides diffusion, there must be another transport mechanism that controls particle infiltration into the low-concentration area. We conjecture that this is the fluid flow induced by a pressure gradient between the high- and low-concentration areas of the system.

To check this hypothesis, we started from detailed analysis of spacial and temporal properties of the “x” component of the velocity vector, $v_x(x, t)$. Figure 3 depicts the velocity profile at several times t . It shows that the region $x > 0$ can be split into two parts characterized by different behavior of v_x . The first region coincides with the particle infiltration area. The system already “feels” the pressure gradient there and responds to it by developing a small but definitely nonvanishing flow towards the low concentration area. The second region is located further away from the infiltration area. The system remains there close to the initial state, with v_x fluctuating around 0.

In order to study the concentration front dynamics, one thus have to take into account the front velocity, v_f . In general, this quantity is both x - and t -dependent. However, we are interested only in its approximate value at time t , and estimate it as a mean weighted with $c(x, t) - c_2$,

$$\bar{v}_f(t) = \frac{\int_0^\infty v_x(x, t)[c(x, t) - c_2] dx}{\int_0^\infty [c(x, t) - c_2] dx}. \quad (4)$$

In this definition we utilize the fact that the weight function quickly vanishes outside the front region (Fig. 2), while the averaged quantity, v_x , remains almost constant there (Fig. 3). Moreover, the integral form of the definition helps to significantly reduce the influence of relatively large statistical noise present in the data for v_x .

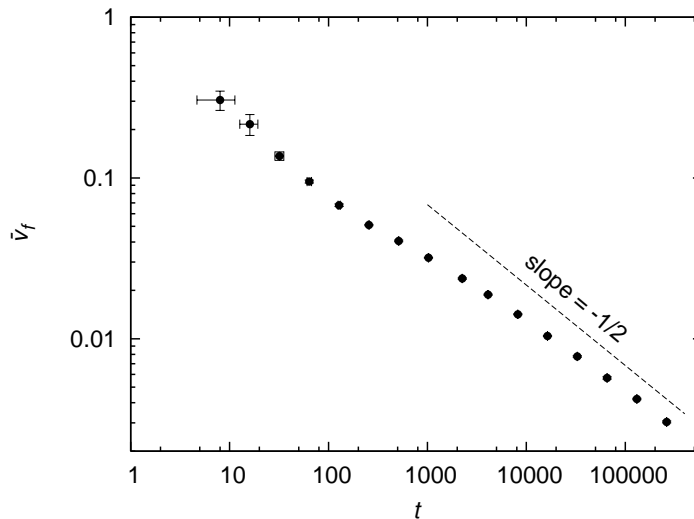


Figure 4. The mean front velocity, \bar{v}_f , as a function of time. The dashed line is a guide to the eye with a slope $-1/2$.

Figure 4 shows that the initial magnitude of \bar{v}_f is very high, almost reaching the maximum possible value 1. At larger times \bar{v}_f decreases as $t^{-\beta}$ with $\beta \lesssim 1/2$ very weakly depending on t . Consequently, the distance the front moves due to the flow,

$$s(t) = \int_0^t \bar{v}_f(\tau) d\tau, \quad (5)$$

for large t grows as $t^{1-\beta(t)}$, i.e. a bit faster than the typical diffusive length $\approx t^{1/2}$. This suggests that the front dynamics is controlled by *both* diffusion and flow. Actually, our simulations showed that after $t = 256000$ time steps the front displacement was $\Delta x \approx 3750$ l.u. (see Figure 2), of which $s(t) \approx 1440$ l.u., that is, about 38%, was caused by the fluid flow.

To separate diffusion from flow, we investigated the front propagation using a mobile reference frame (x', t) , with

$$x' \equiv x - s(t). \quad (6)$$

This new coordinate system moves along the “x” axis with velocity $\bar{v}_f(t)$, so as to minimize effects of the fluid flow. Assuming that in this new reference system the front dynamics is dominated by (normal) diffusion, the concentration profiles should asymptotically obey a similarity relation

$$c(x', t) = f((x' - x_0)/\sqrt{t}), \quad (7)$$

where f is a similarity function and x_0 is a constant. To verify this conjecture, we first used the data for $c(x', t) = 0.5$ to estimate $x_0 \approx -190$, and then plotted c as a function of $(x' - x_0)/\sqrt{t}$ for several times t . The results, obtained for $8000 \leq t \leq 512000$, are shown in Figure 5. They confirm that the concentration profiles asymptotically satisfy (7), as for $t \geq 64000$ the scaled-up profiles are practically indistinguishable.

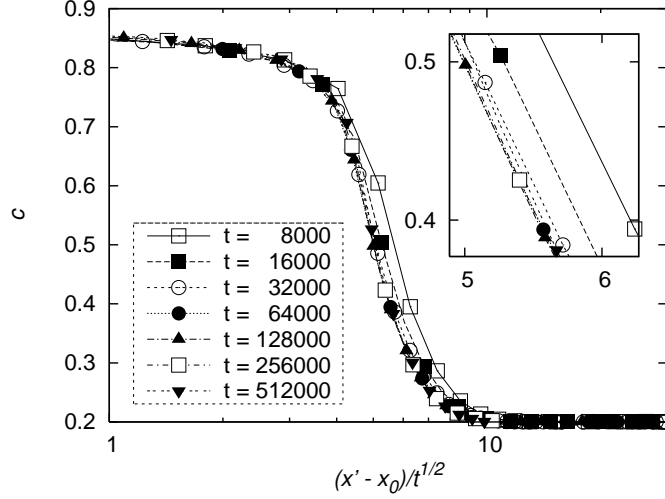


Figure 5. Reduced concentration c as a function of $(x' - x_0)/\sqrt{t}$, with $x_0 = -190$. The inset shows an enlargement of the central part of the main plot, with linear axes.

Hydrodynamical flow can also explain another feature of the model—discontinuity of fluid concentration at the boundary $x = 0$. Even though the boundary condition (2) forces the concentration to be fixed at c_1 for $x < 0$, its values at $x > 0$ are significantly smaller than c_1 (see Figure (2), obtained for $c_1 = 0.9$). Discontinuity in c , Δc , is related to discontinuity in the flow velocity $\Delta v \approx \bar{v}_f$ ($v_x = 0$ for $x < 0$ and $v_x \approx \bar{v}_f$ for $x \gtrsim 0$). Let $c^+ = c_1 - \Delta c$ denote the concentration at $x = 1$ l.u. The rate of diffusive particle transfer per unit length through the interface $x = 0$ is approximately equal to $3c_1 - 3c^+ = 3\Delta c$ (the factor 3 is the number of velocity directions in the LGA model that transfer particles through the interface). This must be balanced by particle current caused by the fluid flow, which can be approximated by $7c^+\bar{v}_f$ (the factor 7 is the number of possible particle velocities). Thus, $3c_1 - 3c^+ \approx 7c^+\bar{v}_f$, or

$$\Delta c \approx \frac{7c_1\bar{v}_f}{3 + 7\bar{v}_f}. \quad (8)$$

Comparison of this formula with the actual data obtained in simulations is shown in Figure (6). The agreement is fairly good.

4. Discussion

Several features of the model deserve closer attention. First, the model employs specular scatterers to mimic a porous medium as well as to reduce hydrodynamic effects [13]. However, the effect of such scatterers on the diffusion along the “x” axis is very peculiar: the “x” component of the momentum is changed only for those particles, whose velocity vector is parallel to the “x” axis. For this reason specular scatterers are widely used in LGA models to implement slip-free walls parallel to the x axis. However, in the KL model the scatterers are distributed randomly with a relatively small concentration to form isolated, point-like islands. Such scatterers are inefficient in breaking temporal

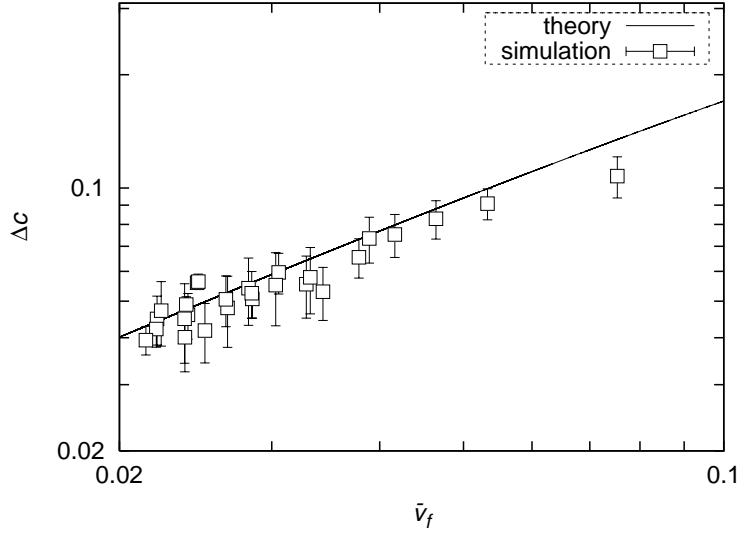


Figure 6. Reduced concentration drop, Δc , at the boundary $x = 0$ as a function of the front velocity \bar{v}_f , obtained from simulations (\square) and equation (8) (solid line).

correlations in the “x” component of momentum of particles that hit them. Thus, on the one hand, randomly distributed specular scatterers have a very limited impact on the diffusivity along the “x” axis. On the other hand, the mean-free path, and hence the diffusion coefficient in the original, scatterer-free FHP model diverge to infinity as the reduced particle concentration goes to 0 or 1 [13]. Combination of these two effects explains the fundamental property of the KL model: extremely strong dependence of the diffusion coefficient on concentration [13].

Second, the present model is based on the FHP model, where particle-particle collisions preserve mass and momentum to mimic fluid flow. Local conservation of momentum leads to hydrodynamic flow from high-pressure (high-concentration) to low-pressure (low-concentration) areas. Therefore, hydrodynamical flow in any FHP-based model of porous media is inevitable and its effects should be always carefully taken into account, especially when specular scatterers are used to model a porous medium.

Third, assume that as soon as the flow velocity in the front becomes sufficiently small, the particle flux q associated with it obeys Darcy’s law [18]

$$q = -\frac{\kappa}{\mu} \nabla P, \quad (9)$$

where κ is the permeability of the medium, μ denotes the fluid viscosity, and ∇P is the pressure gradient. Taking into account that $q \propto v_x$ [18], $\mu \propto D^{-1}$ (Stokes-Einstein relation), and $P \propto c$ [19], one arrives at

$$v_x \propto D \nabla c. \quad (10)$$

If D is very large, even a very small concentration gradient can cause a significant fluid flow. Therefore, one can expect strong hydrodynamical effects to appear in *any* hydrodynamical model of porous medium with diffusion coefficient $D(c)$ diverging to infinity at some value(s) of c .

Fourth, the value of $|x_0|$ in the similarity relation (7) turned out quite large. Similarly, the relaxation time to the asymptotic, long-time regime in which the similarity holds, τ_{relax} , is also large. These two effects may be related to the fact that in all FHP models v_x , which constitutes the left-hand side of relation (10), is limited from above. However, the right-hand side of (10) is a product of two quantities that at early stages of the front propagation assume very large values in the front region. Thus, the system can obey Darcy law only after a long relaxation time necessary to reduce the concentration gradient ∇c to a value of order $1/D$. This explains why in the previous studies the front dynamics was found “anomalous” only if both c_1 was close to 1 and the specular scatterers were used [6, 13, 14]. If any of these conditions was not satisfied, the value of diffusion coefficient D took on relatively small values in the front region and the relaxation time was small enough to allow the simulations to reach the asymptotic regime. Note also that large values of $|x_0|$ and τ_{relax} are in accord with several recent experiments on sorptivity of building materials, where a short-time deviation from the $t^{1/2}$ behavior was found (see [4] and references therein).

Fifth, the actual front velocity at early times turned out smaller than its value extrapolated from the long-time, “Darcy” asymptotics (see Fig. 4). As a consequence, x_0 is negative and the front dynamics at early times appears “superdiffusive” ($\alpha > 1/2$). In systems where the early-time velocity is larger than the short-time extrapolation of the Darcy asymptotics, x_0 would be positive and the early-time front dynamics would appear “subdiffusive” ($\alpha < 1/2$).

Finally, Figure 4 suggests that at large times the mean front velocity, \bar{v}_f , becomes proportional to $1/\sqrt{t}$, which yields a characteristic length scale $\int_{\tau=0}^t 1/\sqrt{\tau} d\tau \propto \sqrt{t}$. This implies that the characteristic lengths associated to both diffusion and fluid flow asymptotically scale with time in the same way, as \sqrt{t} . Consequently, the KL model is an example of a system where measurements based only on analysis of asymptotic concentration profiles cannot differentiate between diffusive and hydrodynamic effects.

5. Conclusions

We have shown that the unusual dynamics of the concentration front in the KL model of a porous medium can be fully explained as a combined effect of hydrodynamic flow and normal diffusion. Our argumentation is not only simpler than that proposed by K untz and Lavall e [6, 13, 14], who used the concept of anomalous diffusion, but also allows to explain more physical properties of the model, e.g. a concentration drop at the boundary $x = 0$.

From our analysis the following picture of the concentration front dynamics in the model emerges. A concentration gradient across the front leads to a pressure gradient which, in turn, forces the FHP fluid to flow. This flow is attenuated by scatterers that mimic a porous medium, so that hydrodynamical effects in most cases are negligible, especially at large times. However, randomly distributed specular scatterers used in the KL model are very inefficient at reduced concentrations close to 1. In this

particular case the viscosity goes to 0, and both diffusivity and mobility along the “x” axis tend to infinity. Under these conditions, hydrodynamical flow significantly affects the front dynamics at all times. In particular, it renders the relaxation time to the asymptotic regime, where Darcy law holds, very large, and significantly changes the position of the Boltzmann-Matano interface x_0 . The front dynamics is controlled by both diffusion and fluid flow, and at very large times the characteristic length scales of both processes become proportional to \sqrt{t} . Consequently, at very large times the concentration profile can be expressed as a function of a single variable x/\sqrt{t} , which could easily be misinterpreted that the front dynamics is governed only by diffusion.

While the KL model cannot be regarded as a model of anomalous diffusion, it remains an interesting model of fluid flow in a porous medium. Its main advantage is ability to reproduce some non-trivial properties of concentration profiles found in several recent experiments. Similarity between the model and experimental results suggests that the anomalous front behavior observed e.g. in experiments on building materials, may have nothing to do with anomalous diffusion, but is caused by some hydrodynamic effects that accompany normal diffusion.

References

- [1] A. El-Ghany El Abd and J.J. Milczarek. Neutron radiography study of water absorption in porous building materials: anomalous diffusion analysis. *J. Phys. D: Appl. Phys.*, 37:2305, 2004.
- [2] L. Pel, K. Kopinga, G. Bertram, and G. Lang. Water absorption in in a fired-clay brick observed by NMR scanning. *J. Phys. D: Appl. Phys.*, 34:675, 1995.
- [3] M. Küntz and P. Lavallée. Experimental evidence and theoretical analysis of anomalous diffusion during water infiltration in porous building materials. *J. Phys. D: Appl. Phys.*, 34:2547, 2001.
- [4] D.A. Lockington and J.-Y. Parlange. Anomalous water absorption in porous materials. *J. Phys. D: Appl. Phys.*, 36:760, 2003.
- [5] A.E. Carey, S.W. Wheatcraft, R.J. Glass, and J.P. O’Rourke. Non-Fickian ionic diffusion across high-concentration gradients. *Water Resour. Res.*, 31:2213, 1995.
- [6] M. Küntz and P. Lavallée. Anomalous diffusion is the rule in concentration-dependent diffusion processes. *J. Phys. D: Appl. Phys.*, 37:L5–L8, 2004.
- [7] G. Rehage, O. Ernst, and J. Fuhrmann. Fickian and non-fickian diffusion in high polymer systems. *Discuss. Faraday Soc.*, 49:208–221, 1970.
- [8] J.D. Fowlkes *et al.* Molecular transport in a crowded volume created from vertically aligned carbon nanofibres: a fluorescence recovery after photobleaching study. *Nanotechnology*, 17:5659, 2006.
- [9] A.T. Lobutets, A.G. Naumovets, and Yu. S. Vedula. Diffusion of adsorbed particles on surfaces with channeled atomic corrugation. In A. Pekalski and K. Sznajd-Weron, editors, *Anomalous Diffusion: From Basics to Applications*, volume 59 of *Lecture Notes in Physics*, pages 340–348. Springer, 1999.
- [10] R. Gomer. Diffusion of adsorbates on metal surfaces. *Rep. Prog. Phys.*, 53:917, 1990.
- [11] D. ben Avraham and S. Havlin. *Diffusion and Reactions in Fractals and Disordered Systems*. Cambridge Univ. Press, Cambridge, 2000.
- [12] R. Metzler and J. Klafter. The random walk’s guide to anomalous diffusion: a fractional dynamics approach. *Phys. Rep.*, 339(1):1–77, 12 2000.
- [13] M. Küntz and P. Lavallée. Anomalous spreading of a density front from an infinite continuous source in a concentration-dependent lattice gas automaton diffusion model. *J. Phys. D: Appl. Phys.*, 36:1135, 2003.

- [14] M. Küntz and P. Lavallée. Numerical investigation of the spreading-receding cycle in a concentration-dependent lattice gas automaton diffusion model. *Phys. Rev. E*, 71:066703, 2005.
- [15] M. Küntz, J.G.M. van Mier, and P. Lavallée. A lattice gas automaton simulation of the non-linear diffusion equation: a model for moisture flow in unsaturated porous media. *Transport in Porous Media*, 43:289, 2001.
- [16] U. Frish, B. Hasslacher, and Y. Pomeau. Lattice-gas automata for the Navier-Stokes equation. *Phys. Rev. Lett.*, 56:1505, 1986.
- [17] J. Crank. *The mathematics of diffusion*. Oxford Univ. Press, Oxford, 1956.
- [18] J. Bear. *Dynamics of Fluids in Porous Media*. Courier Dover Publications, Dover, 1989.
- [19] B. Chopard and M. Droz. *Cellular Automata Modeling of Physical Systems*. Cambridge Univ. Press, Cambridge, 1998.